

# PCCP

Accepted Manuscript



This is an *Accepted Manuscript*, which has been through the Royal Society of Chemistry peer review process and has been accepted for publication.

*Accepted Manuscripts* are published online shortly after acceptance, before technical editing, formatting and proof reading. Using this free service, authors can make their results available to the community, in citable form, before we publish the edited article. We will replace this *Accepted Manuscript* with the edited and formatted *Advance Article* as soon as it is available.

You can find more information about *Accepted Manuscripts* in the [Information for Authors](#).

Please note that technical editing may introduce minor changes to the text and/or graphics, which may alter content. The journal's standard [Terms & Conditions](#) and the [Ethical guidelines](#) still apply. In no event shall the Royal Society of Chemistry be held responsible for any errors or omissions in this *Accepted Manuscript* or any consequences arising from the use of any information it contains.

## $\pi$ -ring currents in doped coronenes with nitrogen and boron: diatropic-paratropic duality.

Inmaculada García Cuesta<sup>a\*</sup>, Barnaby Pownall,<sup>a</sup> Stefano Pelloni,<sup>b</sup> Alfredo M. Sánchez de Merás<sup>a</sup>

<sup>a</sup>Instituto de Ciencia Molecular. Universidad de Valencia. P.O. Box 22085, 46071 Valencia (Spain)

<sup>b</sup>Dipartimento di Scienze chimiche e geologiche, Università degli Studi di Modena e Reggio Emilia. via Campi 183, 41100 Modena (Italy)

### Corresponding Author

\* e-mail: garciain@uv.es

### Abstract

The change of the electronic structure of coronene upon doping with nitrogen or boron has been theoretically studied by means of its magnetic properties and magnetic field induced current density maps. The addition of two atoms of nitrogen or boron to the central ring of coronene causes a drastic variation of the delocalization of  $\pi$ -electrons, which does not depend on its nature but instead on its position. Then, doping in *para* position makes coronene more aromatic while doping in *meta* position makes it to become antiaromatic. Magnetic behavior of the pristine molecule is characterized by two concentric currents flowing in opposite senses that are converted into hemi-perimetric currents in the ortho and meta isomers, so dividing the molecule in aromatic and antiaromatic regions. The paratropic and diatropic ring currents of the coronene moiety may, therefore, be modulated through the position of the heteroatom and, consequently, also the localized/delocalized behavior.

## 1. Introduction

The study of polycyclic compounds that have proven difficult to synthesize has particularly benefited from a growing body of theoretical research in the field. In particular, the electromagnetic properties of these structures have generated intense interest in the scientific community as their potential technological applications have come to light, with a great deal of activity focusing on graphene and graphene-like structures.<sup>1-4</sup> To obtain a certain electrical or optical response from a given material requires a structural change, which in turn can produce a gain or loss of aromaticity in the constituent molecules, and their properties can be easily tuned by means of changes in their  $\pi$ -conjugated structure. The presence of defects, impurities or dopants in planar carbon structures changes the structural and electronic properties substantially.<sup>5-10</sup> So, graphene doped with N or B atoms has been used as an anode in high-potential lithium batteries subject to conditions of rapid charge and discharge, and field effect transistors.<sup>11-12</sup> Furthermore, in another investigation nanoribbons of graphene have had their electronic transport refined by doping with nitrogen and boron.<sup>13</sup> In this context, heteroatom-doped polycyclic aromatic hydrocarbons (PAHs) have become typical models of graphene-like sheets where to investigate structures presenting a certain electric or magnetic response, as these heteroatoms modify the electronic nature keeping the structure.<sup>14</sup>

19

The  $\pi$ -electronic structure of a molecule can be rationalized by means of its response to an external magnetic field in terms of the modulus and direction of the induced currents. Ring currents are deeply linked to the concept of aromaticity and are very useful in the interpretation of the properties of  $\pi$ -conjugated systems. Diamagnetic currents represent the contribution of the  $\pi$ -electrons to diminish the external magnetic field, as characteristic of aromatic systems with delocalized electrons, while paramagnetic currents contribute to increase the external magnetic field as characteristic of antiaromatic systems.<sup>20-23</sup> Hirschfelder<sup>24</sup> has defined them as *subobservables*, since they are not directly observable but can be inferred from magnetic anisotropy and <sup>1</sup>H-NMR spectra data. In particular, high negative values of the magnetic susceptibility and its anisotropy as well as the proton deshielding in the direction of the applied magnetic field are often considered a fingerprint of aromatic systems. Moreover, those quantities are experimentally measurable. Finally, the current density,  $\mathbf{J}(\mathbf{r})$ , is a vector quantity depending of the position in a three-dimensional

space, allowing for the visualization of the electronic structure over the molecule by plotting contour levels, modulus, and streamlines of fields in three dimensions.

From a chemical point of view, coronene is a peri-condensed PAH and can serve as model of graphene sheets and, actually, its structure has been successfully used to investigate the adsorption of hydrogen over graphene.<sup>25</sup> Coronene is considered aromatic because its high negative magnetic anisotropy (-101.6 a.u.) and significant proton deshielding ( $\sigma_{\perp}=-22$  a.u. and chemical shift  $\delta=9$  ppm).<sup>26</sup>

Coronene has a distinctive pattern current generated by the influence of an external magnetic field contrary to that found in benzene, but common to other n-circulene like corannulene.<sup>27</sup> The existence of the two concentric counter-rotating  $\pi$ -rings currents, with a diamagnetic rim and paramagnetic hub, indicates that coronene shows outer aromatic but inner non-aromatic circuits; this current is sensitive to small changes in the structure of the molecule. The substitution of two of the central carbon atoms for two atoms of boron or nitrogen, in the para-, ortho- and meta- position is one such change since B and N are widely used as dopants to tune the physical properties of graphene. Previous studies<sup>14-16</sup> have analyzed the modifications introduced in such rim-and-hub patterns by the substitution of benzenoid carbocycles by isoelectronic borazine units as well as the produced variations in its electronic and magnetic properties. They conclude that the main consequence is the localization of the magnetic response in atomic and oligocyclic circulations.

Here, we study a different form of tuning the electronic structure of coronene by adding or removing two electrons of the  $\pi$  cloud by replacing two carbon atoms by two nitrogens or to borons, respectively. So, this investigation aims to see how the properties of coronene change due to the doping, how its aromatic character changes when electrons are added or removed from the  $\pi$  system of the molecule, and what effect the relative position of the doped atoms may cause.

To the best to our knowledge, the considered molecular systems have not been synthesized yet, but several reports have described the preparation of its aza analogues such as 1,2-diazacoronene,<sup>28</sup> 1,2,7,8-tetraazacoronene,<sup>29</sup> 1,5,9-triazacoronene,<sup>30</sup> even though they all have the heteroatoms in the molecular perimeter. However other types of compounds with the

heteroatom in an inner ring, as e.g. pyrrole-fused azacoronenes, have indeed been synthesized.<sup>17-18</sup> At any rate, we expect that our study can help to give additional light into the domain of PAHs, nanographenes and hetero-graphenes and furthermore be a motivation for the synthesis of the considered species. To this end, the magnetic susceptibility and nuclear magnetic shielding of coronenes doped with boron and nitrogen are analyzed together to give a more complete description of the change of its aromatic character, with the maps of current density providing a more visual way to evaluate the ring currents and how their magnitude, direction and shape change.

## 2. Computational Details

The molecular geometries were determined using density functional theory (DFT)<sup>31</sup> with B3LYP parameterization,<sup>32</sup> employing 6-31G\*\* basis set in all the systems studied, with the exception of ortho-diazacoronene. For this, we use Barone and Adamo's modification of the original functional by Perdew and Wang (mPWPW91)<sup>33</sup> with a 6-311G(d,p) basis set.<sup>34</sup> The optimizations were performed with a symmetry restriction of  $D_{2h}$  for coronene and para analogues, and  $C_{2v}$  for the other systems. Analysis of vibrational frequencies demonstrated that the critical points found on the potential energy hypersurface correspond to true minima. All of this was performed using the Gaussian09 programme.<sup>35</sup> The resultant geometries were used in the subsequent calculations of the magnetic properties and the maps of current density were calculated via four different variations of the Continuous Transformation of the Origin of the Current Density approach<sup>23</sup> (CTOCD) method implemented in the SYSMO package.<sup>36</sup> The selected basis sets were (9s5p2d) for C, N, and B, and (5s2p) for H.<sup>37</sup> The exponents of the polarization functions used were: 1.03670, 0.30708 for the 2d function of C; 1.06000, 0.03250 for the 2d function of N, 1.01600 for the 2d function of B; and 0.85660, 0.19930 for the 2p function of H. Only the most precise results, those from the numeric zero diamagnetic variation of the CTOCD approach (CTOCD-DZ2) are shown. The maps of current density have been obtained via the same variation in an analytic manner (CTOCD-DZ). Complete Active Space Self-Consistent Calculations (CASSCF) using the 6-31G\*\* basis and DALTON code<sup>38-39</sup> were done to find the ground states and possible multireference character of these in all the systems studied. This package was also used to calculate magnetic properties in para-

diazacoronene at the CASSCF level, with 6-31G basis and Gauge-Including Atomic Orbitals<sup>40</sup>  
<sup>31</sup> (GIAO).

### 3. Results and Discussion

#### 3.1. Stability and Magnetic Properties

Doping of coronene with two nitrogen atoms represents 9% in weight and adds 2 electrons to the  $\pi$  system, while doping with two boron atoms represents 7% in weight and withdraws two electrons; in both cases, doping makes the molecules systems to become  $4n+2$  molecular systems. We studied the para-, ortho- and meta-isomers of diboracoronene and diazacoronene, placing the heteroatoms in the central ring of coronene, see Fig. 1.

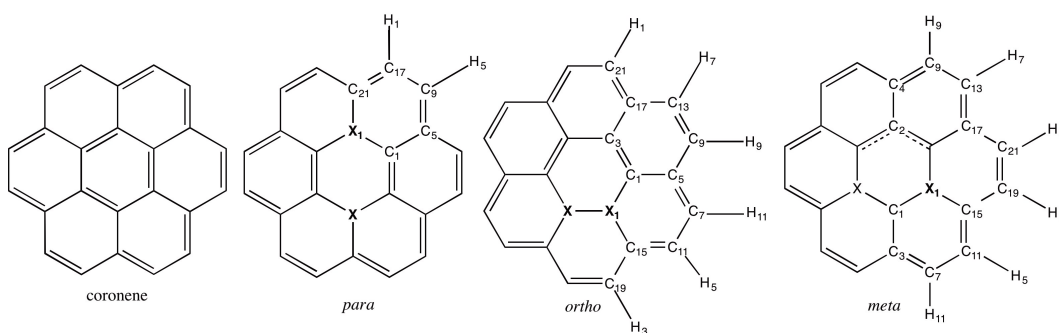


Figure 1. Structure of coronene and para, ortho, and meta disubstituted coronenes. Only symmetry independent atoms are specifically labeled. X=N and B.

The structures with the lowest energy are the ortho- analogues, followed by the para- and meta- isomers, which have very similar energies. Due to the proximity of the lowest singlet and triplet states, the para- isomers show a peculiar electron structure and, in fact, the ground state of para-diboracoronene has triplet multiplicity. Nevertheless, for para-diazacoronene, CASSCF(10,14)/6-31G\*\* calculations give as lowest state the  $^1A_g$  singlet, which presents some multiconfigurational character and is very near the states  $^3B_{2u}$  and  $^1B_{2u}$ . The HOMO-LUMO gap was decreased by doping, and the order of the energy gaps from largest to smallest, is as follows: 1) coronene, 2) ortho-, 3) meta- and 4) para-isomers and in each site the gap is minor with the B-doped than with the N-doped. The calculated values of all the

compounds investigated, as well as those of the isoelectronic species, are given in Table 1. Tada and Yoshizawa<sup>41</sup> have found the same trend in the energy gaps in nanometric graphite sheets doped with B and N and relate the gap decrease to the localization of the  $\pi$ -density caused by the heteroatoms.

The out-of-plane susceptibility ( $\chi_{\perp}$ ) and the magnetic anisotropy ( $\Delta\chi = \chi_{\perp} - \chi_{\parallel}$ ) provide quantitative descriptors of ‘magnetic aromaticity’ (diatropicity) also related to  $\pi$  electron delocalization. Theoretical predictions for all closed shell singlets are shown in Table 1. For triplet states, the spin component is very much larger than the orbital one and consequently we have not considered p-B<sub>2</sub>C<sub>22</sub>H<sub>12</sub>. Furthermore, the large values of the diamagnetic susceptibility obtained for para-diazocoronene at the Coupled Hartree-Fock (CHF) CTOCD-DZ2 level are confirmed by means of multireferential GIAO-CASSCF calculations, in order to give account of the multiconfigurational character mentioned above.

According to well-established magnetic criteria for aromaticity,<sup>23,42-46</sup> para-diazacoronene is found to be more aromatic than coronene and than any of its doped analogues. Ortho-diboracoronene and ortho-diazacoronene are also diatropic, but less than coronene. The meta-analogues, however, show a completely different behavior, with out-of-plane susceptibility  $\chi_{\perp}$  sensibly smaller than in the other derivatives and even smaller than the in-plane components. Consequently, the magnetic anisotropy are positive for both meta-derivatives, as characteristic of antiaromatic compounds. Anyway, the average susceptibility keeps still negative, although very much smaller than in the other derivatives.

In general, the position of the heteroatoms is shown to have a critical influence on the susceptibility, with the para- and ortho-doped analogues displaying magnetic susceptibility characteristic to aromatic compounds, and the meta-doped analogues that of antiaromatic compounds. The nitrogen analogues are slightly less aromatic than the equivalent boron compound within each geometry. The energy gaps and  $\pi$ -localization seem to follow the same trend in the compounds considered, in line with the findings in nanoscale graphite sheets,<sup>41</sup> with the exception of the para-derivatives.

However, the position of the heteroatoms is not the only factor, the number of electrons being also a key aspect. Actually, the species isoelectronic with coronene (i.e. the boron-analogues dications and the nitrogen-analogues dianions) show magnitudes completely similar to those

of coronene, independently of the position of the heteroatom. Nevertheless, these ions present values slightly smaller because of the  $\chi_{\perp}$  component of the tensor. The equivalent analogy is not possible at the CHF level for the isoelectronic species of diboracoronene and diazacoronene, which are the dication and the dianion of coronene, respectively, since the latter show a strong multiconfigurational character.

Table 1. CHF Energy gaps in eV and Magnetic Susceptibility tensors CTOCD-DZ2 in (cgs emu) ppm a.u.<sup>a</sup>  $\perp$  indicate the tensor component out of the plane of the molecule and **av** is the mean value.

	$E_g$	$\chi_{\perp}$	$\chi_{av}$	$\Delta\chi^b$
$C_{24}H_{12}$	8.5	-6849.7	-3123.8	-5588.9
<i>p</i> - $B_2C_{22}H_{12}$	4.5 <sup>c</sup>	---	---	---
<i>p</i> - $N_2C_{22}H_{12}$	4.8	-9079.0	-3914.4(-3847) <sup>d</sup>	-7746.9
<i>o</i> - $B_2C_{22}H_{12}$	6.6	-3444.0	-1852.1	-2387.8
<i>o</i> - $N_2C_{22}H_{12}$	6.9	-2752.8	-1818.3	-1401.8
<i>m</i> - $B_2C_{22}H_{12}$	5.2	-336.9	-811.0	711.3
<i>m</i> - $N_2C_{22}H_{12}$	5.4	982.2	-555.2	2306.1
<i>Iso-electronic species:</i>				
<i>o</i> - $B_2C_{22}H_{12}^{-2}$	6.1	-6167.1	-2839.5	-4991.2
<i>m</i> - $B_2C_{22}H_{12}^{-2}$	6.4	-6459.1	-2947.0	-5268.1
<i>p</i> - $N_2C_{22}H_{12}^{+2}$	8.0	-4183.2	-2173.7	-3014.3
<i>o</i> - $N_2C_{22}H_{12}^{+2}$	7.4	-4053.4	-2131.9	-2882.3
<i>m</i> - $N_2C_{22}H_{12}^{+2}$	8.0	-4539.7	-2292.6	-3370.7

<sup>a</sup> The conversion factor from cgs a.u. per molecule to cgs emu per mole is  $a_0^3 N_A = 8.923\ 8878 \times 10^{-2}$ ; further conversion to SI units is obtained by  $1\ \text{JT}^{-2} = 0.1\ \text{cgs emu}$ . <sup>b</sup>  $\Delta\chi = \chi_{\perp} - \chi_{\parallel}$ . <sup>c</sup> Triplet ground state. <sup>d</sup> GIAO-CASSCF(10,14) calculations.

The shielding of the hydrogen and carbon nuclei of a compound further elaborates the description of the molecule  $\pi$  structure. If the out of plane component of the proton shielding ( $\sigma_{\perp}$ ) is smaller than the in-plane components, this is taken to be an indicator of aromaticity. The hydrogen atoms give us the most reliable description, as they are located

outside of the immediate proximity of the ring currents and do not suffer substantial induction effects. Our theoretical predictions are shown in Tables 2-3.

Table 2: Nuclear magnetic shielding CTOCD-DZ2 in ppm for ortho-diazacoronene, ortho-diboracoronene, coronene and para-diazacoronene

Atom	<i>o</i> -B <sub>2</sub> C <sub>22</sub> H <sub>12</sub>			<i>o</i> -N <sub>2</sub> C <sub>22</sub> H <sub>12</sub>		
	$\sigma_{\perp}$	$\sigma_{av}$	$\delta X^a$ (exp) <sup>b</sup>	$\sigma_{\perp}$	$\sigma_{av}$	$\delta X^a$
<i>B1/N1</i>	130.55	54.09	---	150.68	141.82	---
<i>C1</i>	205.25	52.52	133.08	155.78	47.41	138.19
<i>C11</i>	167.31	55.44	130.16	158.33	64.30	121.30
<i>C15</i>	194.02	41.04	144.56	126.44	44.33	141.27
<i>C19</i>	140.17	30.38	155.22	154.36	95.80	89.80
<i>H1</i>	17.69	23.48	7.66	17.75	23.61	7.53
<i>H3</i>	23.66	24.66	6.48	26.16	27.84	3.30
<i>H5</i>	22.15	24.57	6.57	23.28	25.69	5.45
<i>H11</i>	20.85	24.64	6.50	22.30	25.14	6.00
	C <sub>24</sub> H <sub>12</sub>			<i>p</i> -N <sub>2</sub> C <sub>22</sub> H <sub>12</sub>		
<i>N1</i>	---	---	---	279.92	190.62	---
<i>C1center</i>	207.43	61.08	124.52 (122.6)	196.74	83.75	101.85
<i>C7external</i>	201.31	55.68	129.92 (128.7)	208.19	60.56	125.04
<i>C11</i>	170.05	59.58	126.02 (126.2)	178.82	71.82	113.78
<i>H1</i>	13.30	22.05	9.09 (8.90)	8.31	20.85	10.25

<sup>a</sup>Chemical shifts are referred to the theoretical TMS value  $\sigma(^1H)=31.10$  ppm,  $\sigma(^{13}C)=185.60$  ppm. <sup>b</sup>The values in parentheses are experimental shift mean values [20, 38] and refer to solution (CDCl<sub>3</sub>) data.

Excellent agreement is found in our theoretical CTOCD-DZ2 chemical shifts of coronene with experimental values for <sup>1</sup>H and <sup>13</sup>C NMR measurements in CDCl<sub>3</sub> solution.<sup>26,47</sup> The overall quality of the calculated properties reinforces the conclusion that the basis sets and

level of theory used are satisfactory to describe magnetic properties of these systems. The down-field shift of the out-of-plane component of proton shielding is bigger than those estimated in benzene,  $\sigma_{\perp}^H \approx 20.4$  ppm, in naphthalene,  $\sigma_{\perp}^H \approx 18.5$  ppm<sup>48</sup> or in tetraazanaphthalenes  $\sigma_{\perp}^H \approx 16.8$  ppm.<sup>44</sup> Para-diazacoronene shows the highest values of the magnetic properties in absolute value among all the considered species, including coronene itself: the largest downfield proton chemical shift, the smallest  $\sigma_{\perp}$  and the biggest and most negative  $\chi_{\perp}$ . All these theoretical results prove the enhanced diatropicity of this molecule, indicating that doping in para- position strengthens delocalization and, consequently, aromatic character. Therefore, stability and diatropicity can be conflicting categories for this molecule.

In the ortho-structures two completely different kinds of protons can be identified: those joined to two rings containing the two heteroatoms and those joined to carbon-only rings. The former (H3 and H3') are strongly shielded with chemical shifts appearing at the high values characteristic of alkenes ( $\delta^1\text{H} = 3.3$  ppm); conversely, the latter (H1, H7, H9 and equivalents) are deshielded, showing  $\sigma_{\perp}$  values sensibly lower than the average and chemical shift characteristic of aromatic compounds ( $\delta^1\text{H} \sim 7$  ppm). There exists a third kind of protons, namely those joined to rings with a single heteroatom (H5, H11 and equivalent), which shows intermediate shieldings and shifts. The larger nuclear magnetic shielding of protons or shorter chemical shifts of ortho-diazacoronene in comparison to ortho-diboracoronene result from the lower electron density in the B-containing analogue.

For the meta-isomers it is also possible to distinguish two types of protons on opposite sides of the molecule. The protons joined to N-containing rings are strongly shielded as usual in antiaromatic species while the protons joined to N-free rings are deshielded. The shielding circuit is much larger than the deshielded one, affecting to 8 protons (H1, H3, H5, H11 and equivalents) while the deshielding circuit affects to only 4 protons (H7, H9 and equivalents), oppositely to the ortho-structures. The big shielding perimeter agrees with the strongly paramagnetic values of the magnetic anisotropy found for the meta-isomers, especially when the heteroatom is nitrogen. Therefore, the doping in meta- position makes the system mainly antiaromatic because of the localization of the  $\pi$  density in the vicinity of the heteroatoms.

Table 3: Nuclear magnetic shielding CTOCD-DZ2 in ppm for meta-diazacoronene and meta-diboracoronene

Atom	<i>m</i> -B <sub>2</sub> C <sub>22</sub> H <sub>12</sub>			<i>m</i> -N <sub>2</sub> C <sub>22</sub> H <sub>12</sub>		
	$\sigma_{\perp}$	$\sigma_{av}$	$\delta X^a$	$\sigma_{\perp}$	$\sigma_{av}$	$\delta X^a$
<i>BI/NI</i>	100.66	63.07	---	180.49	103.26	---
<i>C1</i>	192.78	53.54	132.06	64.32	5.27	180.33
<i>C7</i>	147.90	15.73	169.87	151.79	91.72	93.88
<i>C11</i>	153.14	56.63	128.97	147.78	52.39	133.21
<i>C21</i>	143.48	26.55	159.05	160.39	83.30	102.30
<i>H1</i>	27.40	26.54	4.60	29.94	27.47	3.67
<i>H5</i>	28.31	26.81	4.33	32.37	28.28	2.82
<i>H7</i>	24.13	25.52	5.62	25.47	26.17	4.97
<i>H9</i>	22.96	25.11	6.03	23.48	25.38	5.76
<i>H11</i>	29.21	26.15	4.95	32.86	29.60	1.54

<sup>a</sup>Chemical shifts are referred to the theoretical TMS value  $\sigma(^1H)=31.10$  ppm,  $\sigma(^{13}C)=185.60$  ppm.

In general, carbon nuclear magnetic shieldings are not used in the Ring Current Model to rationalize the  $\pi$  electron structure, since it is difficult to find local distinctive contributions as the nuclei are inside the ring currents. Still, it could be stressed that carbon atoms in diazacoronene are prominently more deshielded than in the boron-containing analogue owing to the enormous induction effect of the nitrogens in the vicinity of them, which agrees with studies of similar structures that possess this feature.<sup>43a,46,49</sup> The presence of the doped boron atoms did not appear to have an effect of the same magnitude, although the carbon was found to be slightly deshielded with respect to coronene.

### 3.2. Current Density

Figures 2-3 show the maps of current density induced by a magnetic field acting in a plane perpendicular to the molecular plane ( $z$  direction for coronene and *para*-diazocoronene and  $x$  direction for *ortho*- and *meta*- analogues). The current lines, modulus of the current density, and three-dimensional perspective of the  $\pi$  current, all in a plane  $0.8 a_0$  above the molecular plane, i.e. close to the maximum of the  $\pi$  density, are shown. Diamagnetic circulation is represented as clockwise and paramagnetic circulation as anticlockwise. The contour maps are shown in all cases with a value of  $0.015nc$  cgs-emu au with  $n=1,2,3\dots$  and  $c$  being the speed of light in a vacuum ( $\sim 137.036$  au). Note that 3D maps show a perspective with the molecular plane rotated  $90^\circ$  anticlockwise with respect to the contour 2D maps, in order to illustrate with deeper detail the variation of the intensity of the density current along the molecular structure.

The maps of  $\pi$  current density in coronene show a weak paramagnetic current with maximum intensity of  $0.032c$  a.u. in the molecule's interior, and a large diamagnetic current that flows around the exterior carbons with maximum intensity of  $0.12c$  a.u. consistent with previous investigations on coronene.<sup>14,20,42-45</sup> After doping, only *para*-diazocoronene keeps the main features of the current density maps of the non-doped molecule. It has concentric counter-rotating ring currents, with an intense diamagnetic rim and paramagnetic hub indicating outer very aromatic but inner non-aromatic circuits. The presence of nitrogen atoms in *para*-position intensifies the peripheral diamagnetic current, which is especially intense in the vicinity of the external carbon atoms at the heterocycle rings, where it reaches to  $0.18c$  a.u. In this area, the current density is almost twice larger than in coronene, as can be seen in the 3D perspective of the system. Two diamagnetic circulation islands centered on the nitrogen atoms can be found although with a lower intensity ( $0.8c$  a.u.) than the external currents. The peripheral carbon atoms invert the current in the internal heterocyclic making it paramagnetic as in coronene,<sup>14</sup> but in addition for *para*-diazocoronene electronic density of nitrogen is moved towards the periphery. The intense peripheral diamagnetic current is consistent with the large deshielding of the protons and with the large diamagnetic anisotropy previously found for *para*-diazocoronene, so confirming that doping with nitrogen in *para*-position enhances the aromatic character of the PAH as well as delocalization of  $\pi$ -electrons.

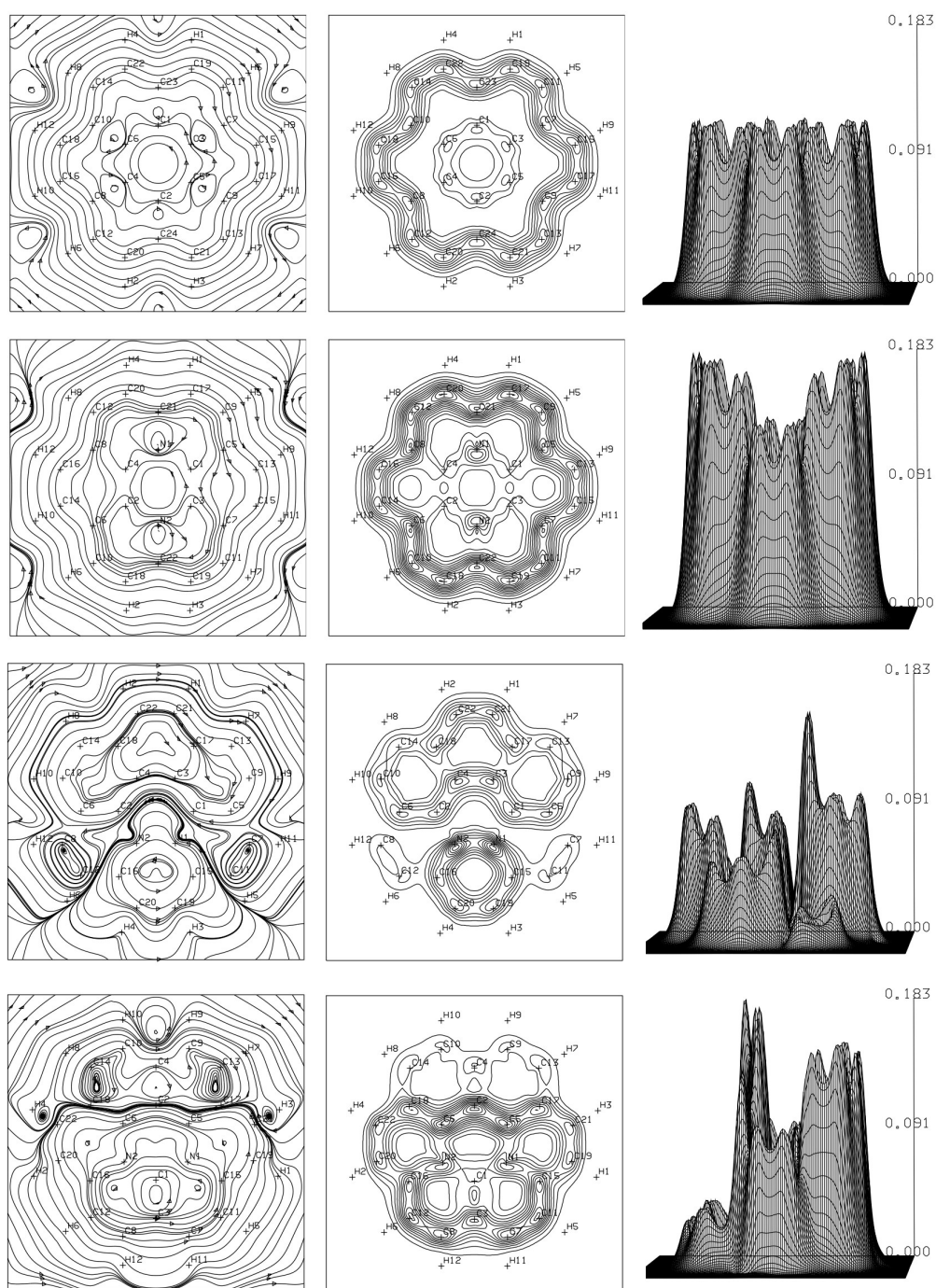


Figure 2. Streamlines of the  $\pi$  current density (left), contour maps for the modulus with values  $0.015nc$ ,  $n=0,1,2,\dots$ , (middle) and 3D-perspective of the maximum ring current on a plane at 0.8 bohr above the molecular plane (right) for coronene, para-, ortho- and meta-diazocoronene (top to bottom). Diamagnetic circulation is clockwise. The maximum  $\pi$  current modulus (contour step) values are 0.12, 0.18, 0.16, 0.18  $c$  respectively, in cgs-emu a.u. In the plots of 3D-perspectives the molecular plane has been rotated  $90^\circ$  anticlockwise to show the zones of lower density.

On the contrary, the  $\pi$  current density maps for the ortho- and meta- isomers are very

different from those of coronene. The presence of the heteroatoms breaks the highly symmetrical ring current found in coronene into distinct parts, reducing the area of the molecule in which the  $\pi$  current density is shared equally, what reflects other findings that explore reductions in symmetry from a highly symmetrical parent molecule.<sup>20,35,43</sup> In the analogues containing heteroatoms in the ortho position it is found a large diamagnetic ring current extending to three carbon rings, which presents a pattern analogous to that of phenanthrene, and a paramagnetic current at the other side of the molecule, extending only along the external ring containing the heteroatoms. The presence of the heteroatoms divides the molecule in two distinct parts: a diatropic one around the carbon rings and a paratropic one around the ring containing the two nitrogens. The currents at both parts have a significant intensity, oppositely to coronene, and are separated by an area with low intensity. Therefore, the interaction with the two nitrogens in ortho-position of the central ring enhances the paramagnetic current of coronene and extends it towards the periphery, making the diamagnetic current to retract at the opposite side.

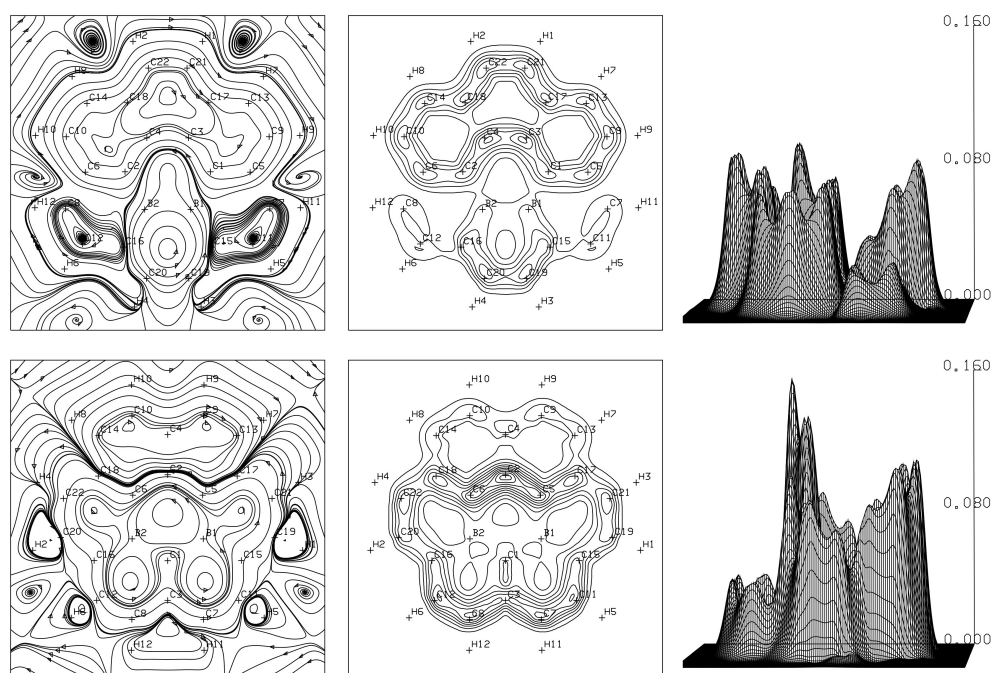


Figure 3.  $\pi$  current density maps for (top to bottom) ortho- and meta-diboracoronene. Streamlines of the current density (left), contour maps for the modulus with values  $0.015nc$ ,  $n=0,1,2,\dots$ , (center) and 3D-perspective on a plane at 0.8 bohr above the molecular plane. Diamagnetic circulation is clockwise. The maximum  $\pi$  current modulus values are 0.095 and 0.160  $c$  in cgs-emu a.u. for ortho- and meta- compounds respectively. In the plots of 3D-perspectives the molecular plane has been rotated  $90^\circ$  anticlockwise to show the zones of lower density.

Some differences are seen comparing the  $\pi$  current density of the N and B doped analogues with ortho geometry. The magnitude and phenanthrene-like shape of the induced diamagnetic ring current is equal; this part of the molecule does not contain a heteroatom, so has an identical structure. However the ring current resembles more closely that found on a phenanthrene molecule<sup>27</sup> in the boron-doped analogue since the intensity of the current is more uniform than in the N-doped isomer. Furthermore, the paramagnetic current found in the nitrogen analogue was found to be significantly larger,  $|J_{\max}|=0.160c$  a.u., centered around the heteroatom-containing lower benzene ring, than the boron analogue  $|J_{\max}|=0.095c$  a.u., reflecting nitrogen's propensity to attract current density towards itself contrary to that the boron. Two additional localized areas, with the shape of the local diamagnetic vortices found in ethylene, are found either side of heteroatom-containing ring in both ortho analogues. They are of relatively very low current density.

In the meta-doped analogues of coronene, heteroatoms again generate two counter-rotating currents that divide the molecule in two parts, as observed in the ortho analogues. However, now the maps representing the  $\pi$  circulation are dominated by a large paramagnetic current ( $|J_{\max}|=0.183$  and  $0.160$  c a.u. for N- and B-compounds, respectively) that runs around all the carbon centers except for the five found at the top of the diagram, i.e. following the perimeter of all the heterocycles. In both cases, the magnitude of the current is greater than the main ring current of coronene and in the opposite direction, being then paramagnetic. The heteroatoms are found in the center of the ring current, the density of which is instead concentrated on atoms C2, C5 and C6, where the visibly weaker diamagnetic current ( $0.03c$  au) and principal paramagnetic current flow together. The diamagnetic ring current surrounding the two carbon-only rings is clearly more delocalized in the boron-containing analogue, whilst the paramagnetic current density is found to be more concentrated on the three aforementioned carbons in the nitro-containing analogue. Then, the occurrence of heteroatoms in five of the seven fused rings allows for the existence of a great paramagnetic circuit, so that the paramagnetic ring currents dominate almost the whole molecule, relegating the very weak diamagnetic current to the two rings placed at the top of the system. The paramagnetic circuits are very similar in the nitrogen and boron meta-doped analogues, since the charge excess of nitrogen is transferred to the neighbor carbon atoms, with no significant maximum being found.

Summarizing, the pattern of the currents induced by an external magnetic field is very different in the ortho and meta-doped isomers from that in the pristine and the para-doped systems. In the former group, induced currents are not counter-rotating concentric currents as in the latter, but hemi-perimetric opposite currents: diamagnetic in the carbon-only rings and paramagnetic in the heterocycles. Therefore, doping in specific positions may divide the system in an aromatic part and an antiaromatic one, whose extension can be moreover be modulated. Obviously, the intensity and direction of the observed ring currents in the studied compounds explain the calculated nuclear magnetic shieldings and the computed susceptibility anisotropies: protons situated in the perimeter of paramagnetic currents present high shieldings. Furthermore, the fact that the diamagnetic current is three times larger than the paramagnetic ones is consistent with the calculated value of its diamagnetic anisotropy.

A different behavior is encountered when the doped analogues (with  $4n+2$  electrons) lose or gain two electrons to become isoelectronic to the parent molecule (with  $4n$  electrons). Then, the position of the heteroatoms is not so relevant, but the number of electrons is determinant instead. Both the dications of the nitrogen-doped systems and the dianions of the boron-doped ones show current patterns very similar to that of the pristine molecule (see Fig. 4): All of them are characterized by two concentric counter-rotating  $\pi$ -rings currents, with a diamagnetic rim and paramagnetic hub. The intensity and the delocalization degree vary depending upon the position and type of heteroatom, although all are slightly less aromatic than coronene. The maps of these systems resembles that of triaza-tribora-coronene (TTC)<sup>14-16</sup>, which is also isoelectronic to coronene. Anyway, the disubstituted systems considered here show the same paramagnetic circulation than coronene instead of the three circulation island around the nitrogen centers found in TTC.

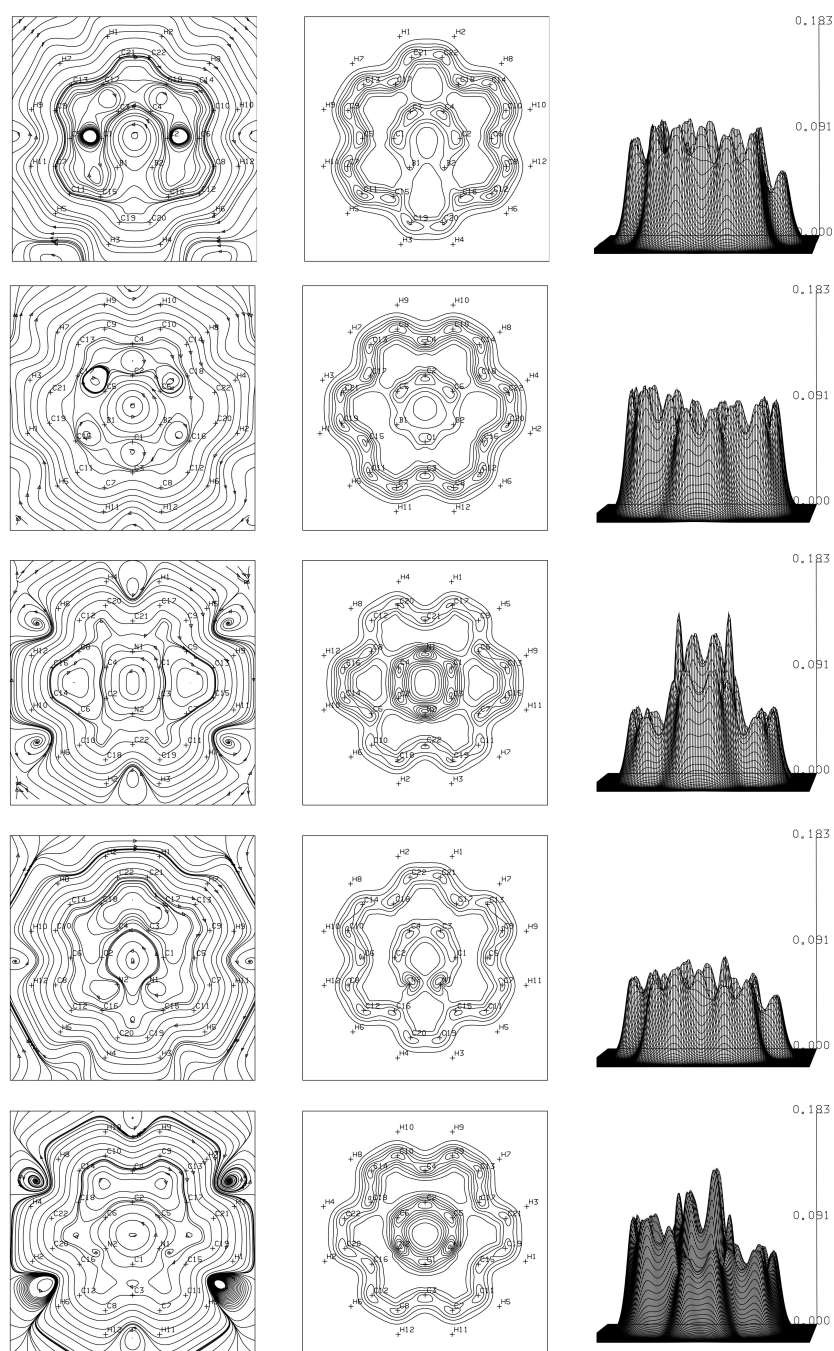


Figure 4.  $\pi$  current density maps for (top to bottom)  $o$ - $B_2C_{22}H_{12}^{2-}$ ,  $m$ - $B_2C_{22}H_{12}^{2-}$ ,  $p$ - $N_2C_{22}H_{12}^{2+}$ ,  $o$ - $N_2C_{22}H_{12}^{2+}$ ,  $m$ - $N_2C_{22}H_{12}^{2+}$ . Streamlines of the current density (left), contour maps for the modulus with values  $0.015nc$ ,  $n=0,1,2,\dots$ , (center) and 3D-perspective on a plane at 0.8 bohr above the molecular plane. Diamagnetic circulation is clockwise. The maximum  $\pi$  current modulus values are (top to bottom) 0.10, 0.11, 0.14, 0.08, 0.14  $c$  in cgs-emu a.u. In the plots of 3D-perspectives the molecular plane has been rotated  $90^\circ$  anticlockwise to show the zones of lower density.

### 3.3. Orbital contributions to the current density

The previous results can be easily rationalized on the basis of symmetry arguments since in the ipsocentric CHF-CTOCD-DZ approach, the current density can be divided in orbital contributions determined by the symmetry properties of translations and rotations. So, the response to a magnetic field can be explained in terms of translation (T) and rotation (R) transitions of the few electrons from the highest occupied orbitals to the lowest virtual orbitals.<sup>42,46-47</sup> As already pointed by Steiner *et al.*<sup>42</sup> the orbitals involved in the coronene  $\pi$ -ring currents are the degenerate highest occupied molecular orbital (HOMO;  $e_{2u}$ , that resolves into  $b_{1u} \oplus a_u$  in  $D_{2h}$ ) and the degenerate lowest virtual molecular orbital (LUMO;  $e_{1g}$ , that resolves into  $b_{2g} \oplus b_{3g}$  in  $D_{2h}$ ). In this way, the most important transitions from occupied to virtual orbitals behave as a translation parallel to the XY molecular plane ( $\Gamma(T_x, T_y) = e_{1u}$ , that resolves into  $b_{2u} \oplus b_{3u}$  in  $D_{2h}$ ) and, consequently, produce diamagnetic contributions.

The case of the azaderivatives is a bit more difficult due to the presence of the extra two  $\pi$ -electrons of the nitrogens atoms. Even though a similar argument can be applied also to the bora-derivatives, now with two electrons less, for the sake of brevity we will restrict ourselves to the case of the nitrogen-doped systems. Firstly, the great difference in orbital energy between HOMO and HOMO+1 (see Fig. 5) makes that the qualitatively most important characteristics of the  $\pi$ -currents can be represented with only the two electrons in HOMO. However, a complete qualitative picture as well as a quantitative description requires the inclusion of six electrons. Furthermore, doping coronene implies the loss of symmetry that goes from  $D_{6h}$  until  $D_{2h}$  for the para- isomer and until  $C_{2v}$  for the ortho- and meta- isomers. Orbital degeneration, then, disappears and HOMO is not degenerate any more and the same happens with LUMO. The HOMOs of the three isomers have symmetry equivalent to the HOMO of coronene, since they come from the stabilization of a virtual orbital of the same symmetry than HOMO. So, HOMO of the para-diaza-coronene behaves as  $b_{1u}$  symmetry class and ortho- and meta- as  $a_2$  symmetry class. Basically, the same happens with the rest of frontier orbitals (see Fig. 5). The rupture of degeneration of the LUMO is larger when the gap is small (para- and meta- analogues) and this, together with the diminution of symmetry explains the different magnetic response of each isomer.

In particular, for para-diazacoronene the six electrons in HOMO ( $5b_{1u}$ ), HOMO-1 ( $2a_u$ ) and

HOMO-2 ( $4b_{1u}$ ) contribute to the  $\pi$  ring currents through transitions to the accessible virtual orbitals LUMO ( $4b_{3g}$ ), LUMO+1 ( $4b_{2g}$ ) and LUMO+4 ( $3a_u$ ). All these transitions behave as translations parallel to the molecular plane ( $\Gamma(T_x) = b_{2u}$  and  $\Gamma(T_y) = b_{3u}$ ). On the other hand, the weak paramagnetic innermost current is associated to the transition  $4b_{1u} \rightarrow 3a_u$ , which presents the same symmetry than a rotation around the field direction ( $\Gamma(R_z) = b_{1g}$ ) and is too energetic to become significant. In addition, we recall that the separation between LUMO and LUMO+1, reminiscent of the coronene LUMO, does not affect significantly the magnetic response, since transitions from HOMO to both virtual orbitals contribute to diamagnetic currents. Consequently, current density maps of the para- isomer shows a pattern very similar to that of the parent molecule.

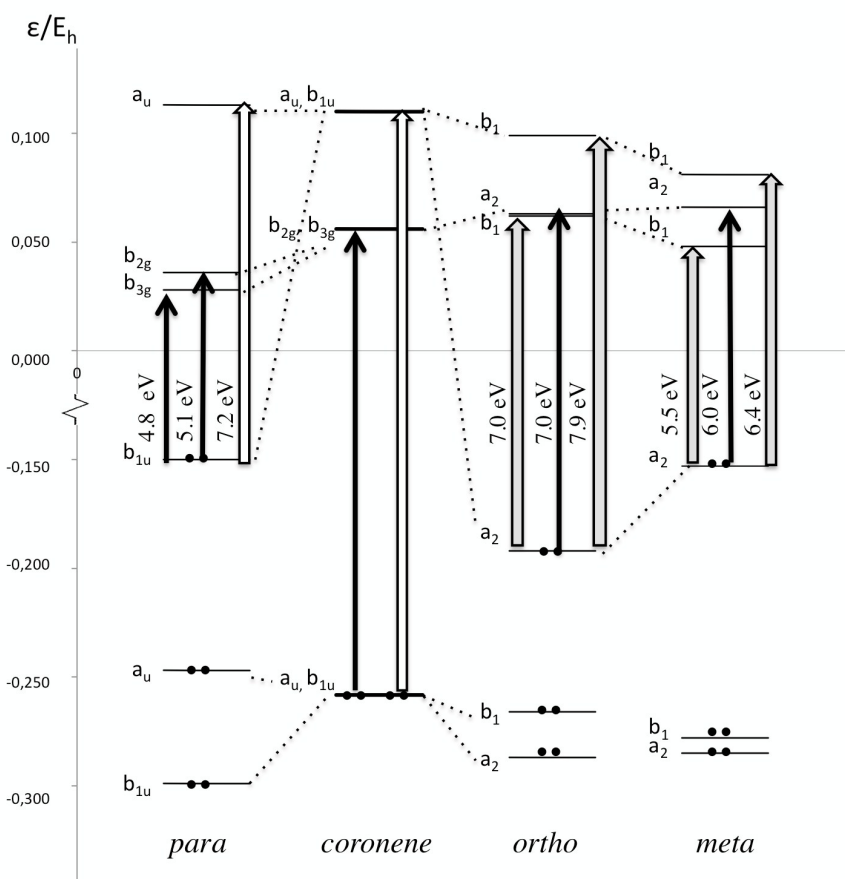


Figure 5. Main orbital contributions to the  $\pi$  ring current in  $D_{2h}$  para-diazacoronene,  $D_{6h}$  coronene, and  $C_{2v}$  ortho- and meta-. The orbital energy level diagram shows the  $\pi - \pi^*$  transitions responsible of the complex pattern of currents in these polycyclic  $\pi$  systems. Black arrows represent translational transitions, white arrows represent rotational transitions and gray arrows represent mixed transitions from occupied levels.

The substitution in ortho- and meta- positions implies a larger loss of symmetry that makes it impossible to reach clear conclusions, since in the  $C_{2v}$  group there are excitations contributing to both paramagnetic and diamagnetic circulations. Still, the fact that in the ortho- and meta- isomers there appear both diamagnetic and paramagnetic sizeable currents can also be rationalized in terms of symmetry arguments, by taking into account that the rupture of degeneration of the coronene LUMO in the meta- isomers are more intense than in the ortho- analogues, diminishing the accessibility of the transition that generates purely diamagnetic currents, what justifies the encountered antiaromatic character. So, the transition from HOMO ( $a_2$ ) to LUMO ( $b_1$ ) is in both cases of  $b_2$  symmetry, which is the symmetry class of translations parallel to the molecular plane ( $T_y$ ) and of the rotations around the magnetic field ( $R_x$ ), giving then both diamagnetic and paramagnetic contributions simultaneously, even though the encountered currents seem to indicate that the paramagnetic contribution dominates at least in the case of the m-diazacoronene. Furthermore, the transition HOMO ( $a_2$ )  $\rightarrow$  LUMO+1 ( $a_2$ ), which behaves like a translational transitions ( $\Gamma(T_z) = a_1$ ), is almost exactly degenerate with the previous one in the case of o-diazacoronene, but rather more energetic for the meta isomer. This different behavior can explain the diamagnetic character of the ortho- derivative and the paramagnetic one of the meta- isomer. The symmetry characteristics of the transitions from HOMO-2 are the same than those just discussed since it is also of  $a_2$  symmetry, while the most important transitions from HOMO-1 ( $b_1$ ) are reversed compared to those from HOMO.

When considering the doped ions, which are isoelectronic to coronene because of the gain or loss of two electrons, the number of low-energy accessible virtual MOs is increased. This allows the existence of transitions contributing to diamagnetic currents that explain the diamagnetic rim. On the other hand, the inner paramagnetic current is reinforced by the transition HOMO-LUMO, which has an intense rotational component.

#### 4. Conclusions

Since diatropicity (*i.e.* magnetic aromaticity) is due to the special mobility of the  $\pi$  electrons

resulting from their delocalization, it can be deduced that doping with nitrogen or boron the central ring of coronene –adding or removing two electrons, respectively– generates a significant change in the delocalization of the  $\pi$ -electrons. The presented calculations reveal that the magnetic response for the doped systems with  $4n+2$  electrons is independent of the absolute number of electrons, but strongly dependent of the position of the doping agent instead. Then, doping in para- position enhances the aromatic character of coronene; in ortho-position, weakens it and, finally, in meta-positions turns it antiaromatic. However, for the corresponding di-ions, which are isoelectronic to the  $4n$ -electrons coronene, the position of the heteroatom is basically irrelevant.

The change in aromatic character is a consequence of the change of  $\pi$ -ring currents on doping, as diatropic and paramagnetic currents of coronene can be activated or deactivated through the regulation of the doping position with nitrogen or boron. Hence, para-diazacoronene shows an enhanced diatropicity compared to the parent molecule (with  $\Delta\chi$  38% larger than coronene), but with the same distinctive pattern of currents: an external intense diamagnetic current and a weak internal one, indicating that innermost  $\pi$ -electrons are localized and outermost delocalized. Conversely, doping in meta- and ortho- position either with nitrogen or boron produces the rupture of the peripheric diamagnetic current of coronene in two currents of opposite directions: one paramagnetic and other diamagnetic. Thus, localized and delocalized circuits are introduced in the molecule, in a way that the system is divided in two parts with very different characteristics and whose area depends on the position of the heteroatoms, making the paramagnetic zone the largest in the meta-analogues and the opposite in the ortho-isomer.

Finally the greatest difference between the nitrogen and boron analogues, in all geometries, is that the localized paramagnetic ring currents in the nitrogen-doped analogues have a higher current density than that of the boron-doped analogues because of the electronic excess in the nitrogen derivatives.

Preliminary calculations on doped circumcoronenes seem to indicate that indeed the aromaticity of graphene sheets can be modulated through doping. Work along this line is in progress and will be object of a subsequent publication.

### Acknowledgements

Authors acknowledge very helpful suggestions by Prof. P. Lazzeretti. This work was supported by the Spanish Ministerio de Economía y Competitividad through project CTQ2010-19738.

### References

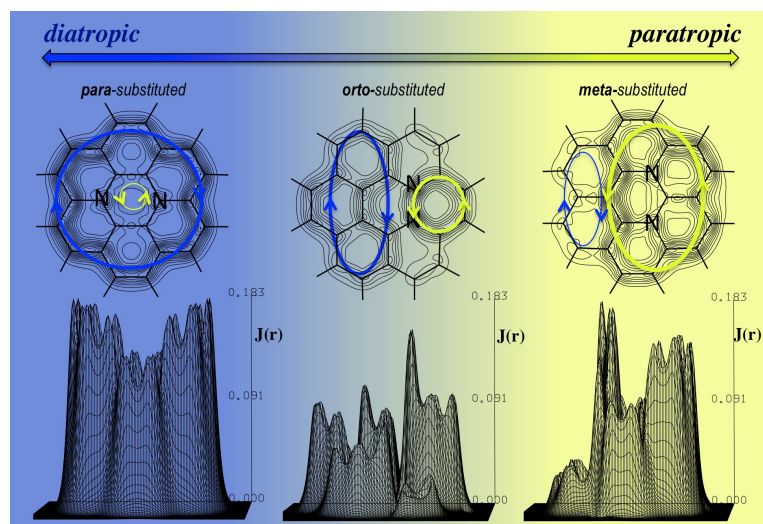
1. A. K. Geim, *Science*, 2009, **324**, 1530.
2. A. H. Castro Neto, F. Guinea, N. M. R. Peres, K. S. Novoselov and A. K. Geim, *Rev. Mod. Phys.*, 2009, **81**, 109.
3. A. K. Geim and K. S. Novoselov, *Nat. Mater.*, 2007, **6**, 183
4. F. Bonaccorso, Z. Sun, T. Hasan and A. C. Ferrari, *Nat. Photonics*, 2010, **4**, 611.
5. Z. F. Wang, Q. X. Li, Q. W. Shi, X. P. Wang, J. L. Yang, J. G. Hou and J. Chen, *Appl. Phys. Lett.*, 2008, **92**, 133114.
6. H. Ren, Q. X. Li, Y. Luo and J. L. Yang, *Appl. Phys. Lett.*, 2009, **94**, 173110.
7. B. D. Guo, Q. Liu, E. D. Chen, H. W. Zhu, L. Fang and J. R. Gong, *Nano Lett.*, 2010, **10**, 4975.
8. K. K. Saha, B. K. Nikolić, V. Meunier, W. C. Lu and J. Bernholc, *Phys. Rev. Lett.*, 2010, **105**, 236803.
9. T. Gunst, T. Markussen, A. P. Jauho and M. Brandbyge, *Phys. Rev. B: Condens. Matter Mater. Phys.*, 2011, **84**, 155449.
10. E. H. Åhlgren, J. Kotakoski and A. V. Krasheninnikov, *Phys. Rev. B: Condens. Matter Mater. Phys.*, 2011, **83**, 115424.
11. A. H. Castro Neto, F. Guinea, N. M. R. Peres, K. S. Novoselov and A. K. Geim, *Rev. Mod. Phys.*, 2009, **81**, 109.
12. Z. F. Wu, W. C. Ren, L. Xu, F. Li, and H. M. Cheng, *ACS Nano*, 2011, **5**, 5463.
13. Y. An, X. Wei and Z. Yang, *Phys. Chem. Chem. Phys.*, 2012, **14**, 15802.

14. E. Steiner, P. W. Fowler, R. G. Vigilione and R. Zanasi, *Chem. Phys. Lett.*, 2002, **335**, 471.
15. P. W. Fowler, C. M. Gibson, and E. L. Nightingale, *Polycycl. Aromat. Compd.*, 2013, **33**, 72.
16. L. Türker, *Polycycl. Aromat. Compd.* 2012, **32**, 61.
17. M. Takase, V. Enkelmann, D. Sebastiani, M. Baumgarten, and K. Müllen, *Angew. Chem. Int. Ed.*, 2007, **46**, 5524.
18. M. Takase, T. Narita, W. Fujita, M. S. Asano, T. Nishinaga, H. Benten, K. Yoza, and K. Müllen, *J. Am. Chem. Soc.* 2013, **135**, 8031.
19. G. Li, W-W Xiong, P-Y Gu, J. Cao, J. Zhu, R. Ganguly, Y. Li, A. C. Grimsdale, and Q. Zhang, *Org. Lett.* 2015, **17**, 560.
20. C.W. Haigh and R.B. Mallion, *Prog. Nucl. Magn. Reson. Spectrosc.*, 1980, **13**, 303.
21. P.J. Garratt, "Aromaticity", Wiley, New York, 1986
22. U. Fleischer, W. Kutzelnigg, P. Lazzeretti, V. Mühlenkamp, *J. Am. Chem. Soc.*, 1994, **116**, 5298.
23. P. Lazzeretti, *Prog. Nucl. Magn. Reson. Spectrosc.*, 2000, **36**, 1.
24. J. O. Hirschfelder, *J. Chem. Phys.* 1978, **68**, 5151.
25. O. Maresca, R. J. -M Pellenq, F. Marrinelli and J. Conard, *J. Chem. Phys.*, 2004, **121**, 12548.
26. E. Steiner, P.W. Fowler and L. W. Jenneskens, *Angew. Chem. Int. Ed.* 2001, **40**, 362
27. G. Monaco, P. W. Fowler, M. Lillington and R. Zanasi, *Angew. Chem. Int. Ed.* 2007, **46**, 1889.
28. S. Tokita, K. Hiruta, K. Kitahara, H. Nishi, *Synth. Commun.* 1982, 229.
29. S. Tokita, K. Hiruta, K. Kitahara, H. Nishi, *Bull. Chem. Soc. Jpn.* 1982, **55**, 3933.
30. . J. Wei, B. Han, Q. Guo, X. Shi, W. Wang, N. Wei, *Angew. Chem., Int. Ed.* 2010, **49**, 8209.
31. R.G. Parr and W. Yang, "Density-Functional Theory of Atoms and Molecules", Oxford University Press, Oxford, 1989.
32. C. Lee, W. Yang and R.G. Parr, *Phys. Rev.* 1988, **37**, 785.
33. J. P. Perdew, in "Electronic Structure of Solids", Ed. P. Ziesche and H. Eschrig (Akademie Verlag, Berlin, 1991) 11; C. Adamo and V. Barone, *J. Chem. Phys.*, 1998, **108**, 664

34. R. Krishnan, J.S. Binkley, R. Seeger and J.A. Pople, *J. Chem. Phys.*, 1980, **72**, 650
35. Gaussian 09, M. J. Frisch, G. W. Trucks, H. B. Schlegel, G. E. Scuseria, M. A. Robb, J. R. Cheeseman, G. Scalmani, V. Barone, B. Mennucci, G. A. Petersson, H. Nakatsuji, M. Caricato, X. Li, H. P. Hratchian, A. F. Izmaylov, J. Bloino, G. Zheng, J. L. Sonnenberg, M. Hada, M. Ehara, K. Toyota, R. Fukuda, J. Hasegawa, M. Ishida, T. Nakajima, Y. Honda, O. Kitao, H. Nakai, T. Vreven, J. A. Montgomery, Jr., J. E. Peralta, F. Ogliaro, M. Bearpark, J. J. Heyd, E. Brothers, K. N. Kudin, V. N. Staroverov, R. Kobayashi, J. Normand, K. Raghavachari, A. Rendell, J. C. Burant, S. S. Iyengar, J. Tomasi, M. Cossi, N. Rega, J. M. Millam, M. Klene, J. E. Knox, J. B. Cross, V. Bakken, C. Adamo, J. Jaramillo, R. Gomperts, R. E. Stratmann, O. Yazyev, A. J. Austin, R. Cammi, C. Pomelli, J. W. Ochterski, R. L. Martin, K. Morokuma, V. G. Zakrzewski, G. A. Voth, P. Salvador, J. J. Dannenberg, S. Dapprich, A. D. Daniels, Ö. Farkas, J. B. Foresman, J. V. Ortiz, J. Cioslowski, and D. J. Fox, Gaussian, Inc., Wallingford CT, 2009.
36. P. Lazzeretti and R. Zanasi, *Phys. Rev.*, 1985, **32**, 2607
37. F. B. van Duijneveldt, "Gaussian basis sets for the atoms H-Ne for use in molecular calculations", Research Report RJ 945, IBM, 1971
38. K. Aidas, C. Angeli, K. L. Bak, V. Bakken, R. Bast, L. Boman, O. Christiansen, R. Cimiraglia, S. Coriani, P. Dahle, E. K. Dalskov, U. Ekström, T. Enevoldsen, J. J. Eriksen, P. Ettenhuber, B. Fernández, L. Ferrighi, H. Fliegl, L. Frediani, K. Hald, A. Halkier, C. Hättig, H. Heiberg, T. Helgaker, A. C. Hennum, H. Hettema, E. Hjertenæs, S. Høst, I.-M. Høyvik, M. F. Iozzi, B. Jansik, H. J. Aa. Jensen, D. Jonsson, P. Jørgensen, J. Kauczor, S. Kirpekar, T. Kjærgaard, W. Klopper, S. Knecht, R. Kobayashi, H. Koch, J. Kongsted, A. Krapp, K. Kristensen, A. Ligabue, O. B. Lutnæs, J. I. Melo, K. V. Mikkelsen, R. H. Myhre, C. Neiss, C. B. Nielsen, P. Norman, J. Olsen, J. M. H. Olsen, A. Osted, M. J. Packer, F. Pawłowski, T. B. Pedersen, P. F. Provasi, S. Reine, Z. Rinkevicius, T. A. Ruden, K. Ruud, V. Rybkin, P. Salek, C. C. M. Samson, A. Sánchez de Merás, T. Saue, S. P. A. Sauer, B. Schimmelpfennig, K. Snegov, A. H. Steindal, K. O. Sylvester-Hvid, P. R. Taylor, A. M. Teale, E. I. Tellgren, D. P. Tew, A. J. Thorvaldsen, L. Thøgersen, O. Vahtras, M. A. Watson, D. J. D. Wilson, M. Ziolkowski, and H. Ågren, "The Dalton quantum chemistry program system", *WIREs Comput. Mol. Sci.* 2014, **4**, 269.
39. Dalton, a molecular electronic structure program, Release DALTON2013.1 (2013), see <http://daltonprogram.org>.

40. K. Ruud, T. Helgaker, R. Kobayashi, P. Jørgensen, K. L. Bak, H.J.Aa. Jensen, *J. Chem. Phys.* 1994, **100**, 8178.
41. T. Tada and K. Yoshizawa, *J. Phys. Chem. B*, 2003, **107**, 8789.
42. W. H. Flygare, *Chem. Rev.*, 1974, **74**, 653.
43. a) I. G. Cuesta, R. S. Jartín, A. Sánchez de Merás and P. Lazzeretti, *J. Chem. Phys.*, 2003, **119**, 5518; b) *J. Chem. Phys.*, 2004, **120**, 6542 ; c) *Mol. Phys.* 2005, 103, 789.
44. I. G. Cuesta, A. Sánchez de Merás and P. Lazzeretti, *J. Comput. Chem.*, 2006, **27**, 1980.
45. I. G. Cuesta, A. Sánchez de Merás, and P. Lazzeretti, *J. Comput. Chem.*, 2006, **27**, 344.
46. I. G. Cuesta, A. Ligabue, A. Sánchez de Merás and P. Lazzeretti, *Chem. Phys. Lett.*, 2005, **401**, 282.
47. M. Jonathan, S. Gordon and B. P. Dailey, *J. Chem. Phys.*, 1962, **36**, 2443.
48. I. G. Cuesta, A. Sánchez de Merás, S. Pelloni and P. Lazzeretti, *J. Comput. Chem.*, 2009, **30**, 551.
49. I. G. Cuesta, J. Sánchez Marín and A. Sánchez de Merás, *Phys. Chem. Chem. Phys.*, 2009, **11**, 4278
50. E. Steiner, P. W. Fowler, R. G. Vigilione and R. Zanasi, *Chem. Phys. Lett.*, 2002, **335**, 471.
51. E. Steiner, P. W. Fowler, R. W. A. Havenith, *J. Phys. Chem. A* 2002, **106**, 7048.
52. A. Soncini, E. Steiner, P. W. Fowler, R. W. A. Havenith, and L. W. Jenneskens, *Chem. Eur. J.*, 2003, **9**, 2974.
53. A. Ciesielski, M. K. Cyrański, T. M. Krygowski, P. W. Fowler and M. Lillington, *J. Org. Chem.* 2006, **71**, 6840.
54. S. Fias, P. W. Fowler, J. L. Delgado, U. Hahn and P. Bultinck, *Chem. Eur. J.* 2008, **14**, 3093.
55. E. Steiner, P. W. Fowler, *J. Phys. Chem. A*, 2001, **105**, 9553; *Chem. Commun.* 2001, 2220.
56. E. Steiner, A. Soncini and P.W. Fowler, *J. Phys. Chem. A* 2006, **110**, 12882.

Abstracts for the Table of contents entry.



By means of doping with nitrogen or boron in the central ring of coronene, it is possible to modulate the size and intensity of the diamagnetic and paramagnetic  $\pi$  ring-currents originated by an external magnetic field and then to switch from delocalized (aromatic) to localized (antiaromatic) behavior.